Hindawi
International Journal of Chemical Engineering
Volume 2023, Article ID 1445360, 11 pages
https://doi.org/10.1155/2023/1445360

Research Article

Development of Alumina-Titania Composite Layers on Stainless Steel through the Detonation Spray Method and Investigation of Salt Spray Corrosion Behavior along with Surface Examination

A. Surya,[1] **R. Prakash**,[1] **P. Senthil Kumar**,[2,3] **and G. Bharath Balji**[2,3]

[1]*Department of Mechanical Engineering, Sri Sivasubramaniya Nadar College of Engineering, Kalavakkam 603110, Tamil Nadu, India*
[2]*Department of Chemical Engineering, Sri Sivasubramaniya Nadar College of Engineering, Kalavakkam 603110, Tamil Nadu, India*
[3]*Centre of Excellence in Water Research (CEWAR), Sri Sivasubramaniya Nadar College of Engineering, Kalavakkam 603110, Tamil Nadu, India*

Correspondence should be addressed to R. Prakash; prakashr@ssn.edu.in and P. Senthil Kumar; senthilkumarp@ssn.edu.in

Received 24 April 2023; Revised 23 June 2023; Accepted 26 June 2023; Published 4 July 2023

Academic Editor: Ho SoonMin

Almost every metal and alloy corrodes when used in high-temperature applications. To combat this problem, ceramic coatings on the metals can be deposited for better thermal and corrosion behavior. The present study applies an alumina-titania (Al_2O_3-TiO_2) ceramic coating to the stainless steel (SS) surface using a detonation spray process. The surface of the coated SS is probed by optical microscopy (OM), scanning electron microscopy (SEM), and X-ray diffraction (XRD). The clear differences between coated and uncoated SS have been observed based on the SEM images. The XRD pattern indicates that the Al_2O_3-TiO_2 coating on SS has been successfully deposited. The hardness of coated and uncoated SS surfaces is determined by using the Micro Vickers hardness tester, which claims that the hardness of the SS surface has decreased after coating. Salt spray tests were used to examine the corrosion behavior of coated and uncoated SS after 12 and 24 hours. After 12 hours, no corrosion was observed on the SS. After 24 hours, however, significant corrosion of uncoated SS is observed, and the coated SS shows negligible corrosion. Based on the study, it is claimed that an Al_2O_3-TiO_2 coating on SS has improved its corrosion behavior significantly.

1. Introduction

Stainless steel is widely used for domestic and industrial applications due to its high corrosion resistance in a variety of harsh environments [1]. However, the usage of stainless steel for its applications is limited by the intermittent nature of high-temperature corrosion. Corrosion in SS components causes adverse effects and premature failure of the components. To avoid the corrosion problem in steel, various coating materials are used. However, a ceramic coating is efficiently used to combat this problem [2–5]. Though ceramic coating has many advantages, it has not entered the commercial market successfully due to its typical coating process. The most significant disadvantage of ceramic coatings, in general, is their lack of self-healing properties. It is an intimidating problem, especially since in-core components such as fuel cladding are subjected to extreme temperatures [6].

To improve the efficiency of ceramic material application, ceramic composite coatings have been successfully used. The corrosion resistance of the substrate was significantly influenced by the various coatings and materials used during the coating process, as evidenced by their performance in a salt spray corrosion test environment under different conditions. The choice of materials and application techniques played a crucial role in determining the level of protection against corrosion. Chromium 20 nickel [7, 8], FeCoCrAlNiTix (x: molar ratio, $x^{1/4}$ 0.5, 1.0, 1.5, and 2.0) [9], tungsten carbide and chromium carbide [10], TiNbMoMnFe high entropy alloy coating [11], sample 316L austenitic

stainless steel [12], nanomodified silicon-based composite coating [13], tube-fitting nuts made of AISI [14], Mg-*X* alloys (*X* = Mn, Sn, Ca, Zn, Al, Zr, Si, Sr) [15], titanium nitride [16], arc sprayed aluminum coating [17], $Fe_{66}Cr_{10}Nb_5B_{19}$ metallic glass coating [18], and titania coated α-Al_2O_3 platelets [19] are some of the examples. Based on the discussion, it is found that ceramic composite coatings are good for use against corrosion. One of the ceramic composite coatings that can be used for the abovesaid purpose is alumina-titania coatings. These coatings are used in textile manufacturing components, tooling, chemical industry components, and electrical insulation due to their high wear resistance, toughness, and good grinding ability [20]. Also, the alumina-titania coating has not been used for improving the corrosion resistance of SS. According to Djendel et al., alumina-titania coatings with an intermediate bond coat of $Ni_{20}Cr_6Al$, deposited on stainless steel substrates using atmospheric plasma spraying, exhibit desirable coating characteristics, including adhesion strength [21].

There are various coating methods for steel; however, thermal spraying is one of the best methods for high-temperature applications. The substrates (base material), coating materials, coating processes, and conclusions are summarized in Table 1. It is observed from Table 1 that detonation gun thermal spraying is one of the compelling methods to coat steel, which may give good corrosion resistance and adhesive strength to steel.

The specific novelty of this study is to investigate the corrosion behavior of 304 stainless steel using an advanced thermal spraying technology called detonation gun spraying. A unique aspect of this research involves applying a 1 : 1 ratio (i.e., 50% wt. of each material) of Al_2O_3-TiO_2 on the stainless steel surface, whereas most of the studies involved a maximum of 40% wt. of TiO_2.

This study uses the detonation gun spray coating technique to coat Al_2O_3-TiO_2 on stainless steel. OM and SEM have found the surface morphologies, while XRD is used to confirm the alumina-titania coating on the SS. The corrosion resistance of SS has been tested under a 5.2% NaCl spray condition. The hardness of the coated and uncoated steels is also investigated in this study.

2. Materials, Instruments, and Methodology

In this study, 304 grade stainless steel was used as a substrate. The percentages of various elements in 304 grade stainless steel are tabulated in Table 2. The coating of alumina-titania powder (50 : 50 by weight) on stainless steel was carried out using the detonation gun spray method. Alumina-titania powder of analytical grade with a purity of 99.5% was purchased for this thermal spray coating method. The experimental arrangement of the detonation gun spray coating method (D-gun spraying) is shown in Figure 1. The coating was carried out by Lotus Surface Technologies Pvt. Ltd., Chennai. Before coating, stainless steel was machined to the required dimensions (80 mm × 60 mm × 10 mm). The selected powder was sprayed on the material with the help of three inert gases. Process parameters for detonation spraying are tabulated in Table 3.

SEM of VEGA3-TESCAN for surface, EV018 (CARL ZEISS) for cross section, and PANalytical X'pert powder XRD system were used to examine the surface. The optical microscope images were recorded with the Dewinter Optical, Inc. microscope. The coated steel underwent the salt spray corrosion test to visually examine the corrosion rate of the coated and uncoated steel surfaces. The salt spray test was conducted according to the ASTM B117-16 standard. The coated and uncoated steel samples were placed in the chamber, and NaCl salt was sprayed rapidly on the steel. The corrosion was tested for two-time intervals: 12 hours and 24 hours. The test parameters are tabulated in Table 4.

The hardness testing of the surfaces was performed as per the IS 1501-13 (P1) standard by using Vicker's hardness tester, Wolpert.

3. Results and Discussion

The actual images of SS and coated SS surfaces are shown in Figures 2(a) and 2(b). The coating on SS was clearly observed in the images through different surface textures.

3.1. SEM, X-Ray Diffraction, and Hardness Analysis of the Surface. The SEM of SS shown in Figure 3 revealed that the marks and pits were present on the surface; however, the surface still looked free from any additional layers of contaminants.

Figure 4 represents the after-coating surface of stainless steel. A covering of SS can be observed in Figures 4(a) and 4(b) after comparison with Figure 3(a). It was evident that the SS surface became rougher and more granular after the alumina-titania coating. The clusters in the coating were more prominently observed in the images shown in Figures 4(c) and 4(d). Thus, it was confirmed through SEM images that an alumina-titania coating was successfully developed on SS through D-gun spray coating.

The cross-sectional SEM morphology with EDX is shown in Figures 5 and 6. It is observed from the figures that the coating is deposited on the substrate and that the respective elements values are found by the EDX spectra, and the respective elemental values are tabulated in Table 5.

Figure 7 shows the XRD diffraction peaks for alumina-titania coated SS. An intense peak was recognized around 22° due to the alumina-titania coating [33]. The peaks of 33° and 50° could also relate to the alumina-titania coating. This fact indicated that alumina and titania interacted with each other to form an alumina-titania composite. Besides alumina-titania, alumina, titania, and SS could also be detected in the coating through their peaks [34]. This fact revealed that some alumina and titania could not react with each other and remain in their original form. Based on XRD peaks, it could be claimed that alumina-titania was successfully coated on SS through D-gun spraying. The XRD analysis of the coated material, Al_2O_3-TiO_2, which consists of alumina (JCPDS card number: 10-173) and titania (JCPDS card number: 21-1276), confirms the successful deposition of the coating on the SS 304 substrate. Figure 7 illustrates the corresponding HKL values (Miller indices).

Table 1: Thermal spray coatings of different materials on various substrates.

Base materials	Substance applied	Coating process	Inference	Reference
Boiler steel	Ni-20 Cr	Detonation spraying	The coating demonstrated significant resistance to oxide scale spallation during cyclic exposures	[7]
S355 steel	Tungsten carbide, chromium carbide, and aluminum oxide	High-velocity oxy-fuel	WC-CoCr provides better protection than uncoated steel, whereas Al_2O_3 provides poor protection	[22]
Hydroturbine steel	Nickel-based coatings	High-velocity flame spray	TiO_2 and Al_2O_3 intense splats were observed evenly. According to micrographs, the interface between the substrate and the coatings was free of breaks	[23]
13Cr4Ni steel	Ni-Al_2O_3 coatings	High-velocity flame spray	Ni-Al_2O_3 coating composition with 40 wt. % Al_2O_3 demonstrated the best resistance to slurry erosion	[24]
17-4 pH stainless steel	Zinc followed by stearic acid	Electrodeposit ion	The coating, as received 17-4 pH stainless steel sample in a simulated seawater medium, demonstrated enhanced coating adhesion and corrosion resistance than other fabricated surfaces	[25]
Invar steel substrates	Fe-based amorphous coating	D-gun spraying and then cryogenic cycling treatment (CCT)	CCT improves the fracture toughness of Fe-based amorphous coatings, the coatings' ability to resist crack transmission improves significantly, allowing the coatings' wear resistance to improve significantly	[26]
Martensitic stainless steel	86WC-10Co-4Cr and 75Cr_3C_2-25NiCr	D-gun spraying	The 75Cr_3C_2-25NiCr coating on martensitic stainless steel has more wear resistance than cumulative weight loss	[27]
Boiler tube steel	10, 20, and 35 wt% of Cr_3C_2 in NiCr	High-velocity oxy-fuel	All the coatings on the ASME SA213 T-22 used for the investigation proved corrosion resistance after being exposed to a destructive Na_2SO_4-V_2O_5 solution in the furnace for 50 hours at 800°C	[28]
Carbon steel substrates	Fe-Cr-Nb-B alloys	Detonation spraying and spark plasma sintering	Due to small particle bonding strength and incomplete crystallization, which concentrated the consolidated material incompetent of sustaining appreciable plastic deformation, the wear resistance of the sintered $Fe_{66}Cr_{10}Nb_5B_{19}$ alloy was lower than that of the $Fe_{66}Cr_{10}Nb_5B_{19}$ DS coatings	[29]
Stainless steel substrates	SS 444 and SS 316	High-velocity oxy-fuel	The lack of protective passivity in thermal spray coatings is primarily inherited from the atomized powdered stainless steel material	[30]
12Ch18N10 T steel	Al_2O_3 coatings	Detonation spray	Ensuring high hardness and wear resistance of the D-gun spraying of Al_2O_3 coating, the volume fraction of α-Al_2O_3 must be increased	[31]
Al_2O_3/Al cored wires	Marine steels	Arc spraying	The enhanced tribocorrosion resistance of the Al-20 percent Al_2O_3 coating is due to the Al matrix's high hardness in the layer, greater load-bearing capacity, compact structure, and superior wear-induced corrosion resistance	[32]

Table 2: Chemical composition of 304 grade stainless steel.

Elements	Percentage
Chromium (Cr)	18
Silicon (Si)	0.75
Nickel (Ni)	0.1
Molybdenum (Mo)	3
Manganese (Mn)	0.75
Sulphur (S)	0.03
Nitrogen (N)	0.1

Figure 1: Experimental arrangement of the D-gun spray coating method.

Table 3: Process parameters of D-gun coating.

Description	Range value
Coating powder	Alumina-titania (Al_2O_3-TiO_2)
Job distance	180 mm
Detonation spraying	3 shots/second
Velocity	1500 m/s
Thickness	300 microns
Inert gas 1 (oxygen)	2 bars
Inert gas 2 (acetylene)	1.5 bar
Inert gas 3 (nitrogen)	3 bars

Table 4: Test parameters of the salt spray test.

Description	Range value
The concentration of salt	5.2% of NaCl
Chamber temperature	33.9°C–34.8°C
The pH of the salt solution	6.8
Air pressure	15 psi (1.034 bar)
Collection of solution per hour	1.2 ml
Exposure period	24 hours

The XRD plot for the corroded sample is analyzed by using a BURKER ECO D8 Advance instrument. The peaks at 16°, 43°, and 74° could also relate that corrosion occurred on the SS 304 sample. The XRD pattern of corroded SS 304 is shown in Figure 8. Figure 8 reveals the composition of corroded SS 304, which includes Cr_2O_3 (JCPDS card number: 76-0147), Fe_2O_3 (JCPDS card number: 73-0603), and Mn_2CrO_4 (JCPDS card number: 36-0546). The corresponding HKL values obtained from Figure 8 provide evidence supporting the occurrence of corrosion on the SS 304 substrate.

The hardness numbers of the coated and uncoated steel are shown in Figure 9. The values are in VHN (Vickers hardness number), and the Rockwell hardness number denotes the equivalent hardness number. It is evident from the results that the hardness of the coated surface is increased by 43.51% than the uncoated surface. It could indicate that an alumina-titania coating was successfully deposited on SS through D-gun spraying. However, surprisingly, the hardness of the coated surface went down with respect to SS instead of increasing. It is evident in Figure 4 that the coating is applied uniformly by the D-gun spray method and that roughness was also greater with respect to the SS surface. Due to this, the hardness of the coated stainless steel is reasonably increased by the alumina-titania coating.

3.2. Salt Spray Corrosion Test. Before the test, the specimen was cleaned gently before loading. Then, the sample was washed in a considerate manner with clean running water to remove testing salt deposits from their surfaces and dried immediately. The obtained results are tabulated in Table 6. The observations were conducted at 12 h intervals and 24 h intervals during the salt spray test. This selection of intervals allowed for better monitoring of corrosion behavior and quicker evaluation of material performance, as one year in the test is equivalent to one year in normal atmospheric conditions [35, 36].

It was important to mention that both coated and uncoated SS did not show corrosion after 12 h. After 24 h, it was observed that uncoated SS showed some corrosion products formed on its surface. On the other side, very few (negligible) corrosion products were observed on the surface of coated SS after 24 h (Figure 8). Thus, it was evident from the salt spray test that the coated SS showed better corrosion resistance than the uncoated SS [37, 38].

A simple immersion test was also performed after this. Both coated and uncoated SS were immersed in 0.5 M NaCl solutions for 24 h. Afterward, they were cleaned and dried, and optical images were clicked. The microscopic images are shown in Figure 9.

It is evident in Figure 10(a) that the uncoated SS had some scratch marks on it. After 24 h immersion, corrosion products formed on the clear surface in Figure 10(b). In the comparison of Figures 10(a) and 10(c), it could be observed that a layer had covered the SS surface. It could indicate that an alumina-titania coating was there. After 24-hour

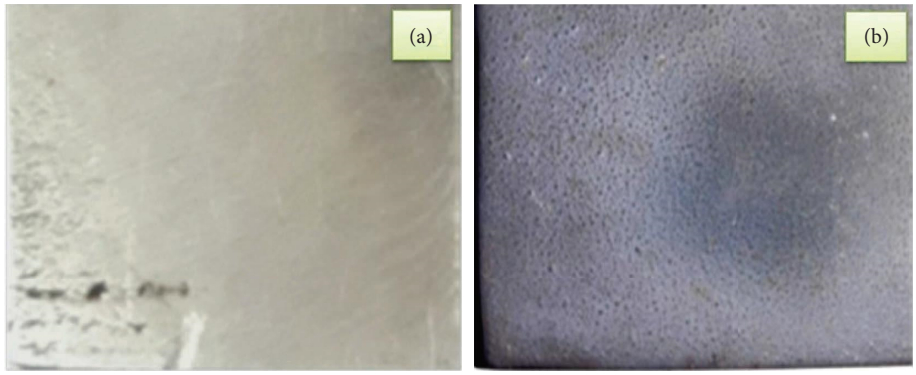

Figure 2: Images of (a) stainless steel and (b) coated stainless steel.

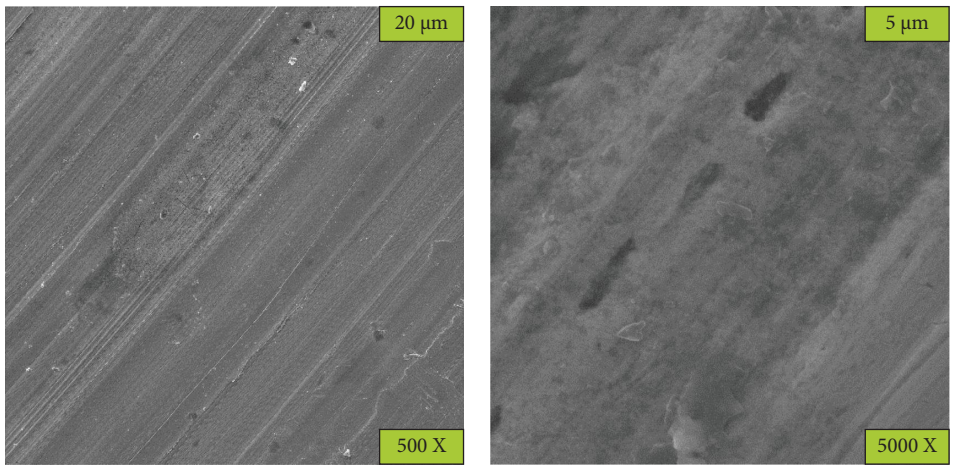

(a) (b)

Figure 3: SEM images of uncoated stainless steel at (a) 500X and (b) 5000X.

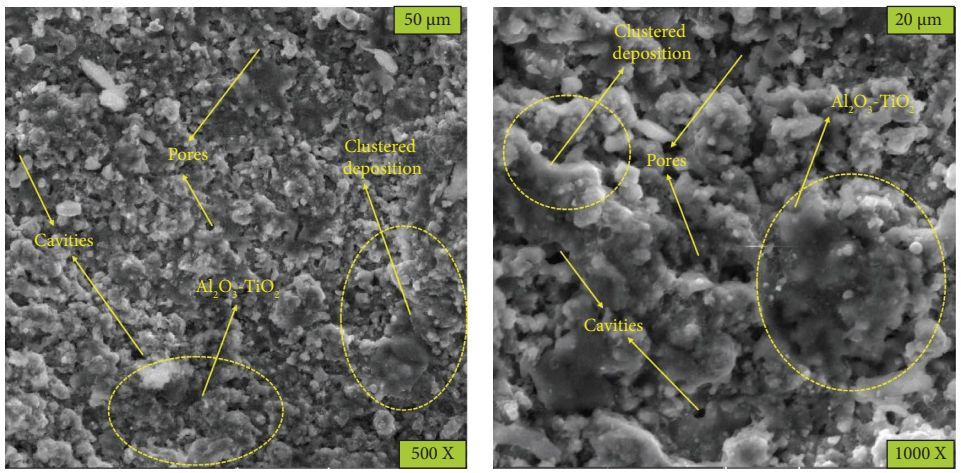

(a) (b)

Figure 4: Continued.

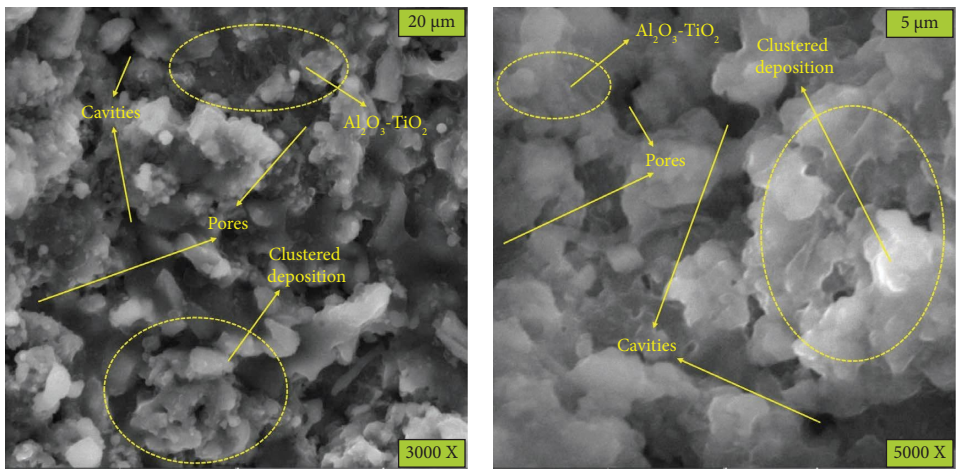

(c) (d)

Figure 4: SEM morphologies of coated stainless steel. (a) 500X; (b) 1000X; (c) 3000X; (d) 5000X.

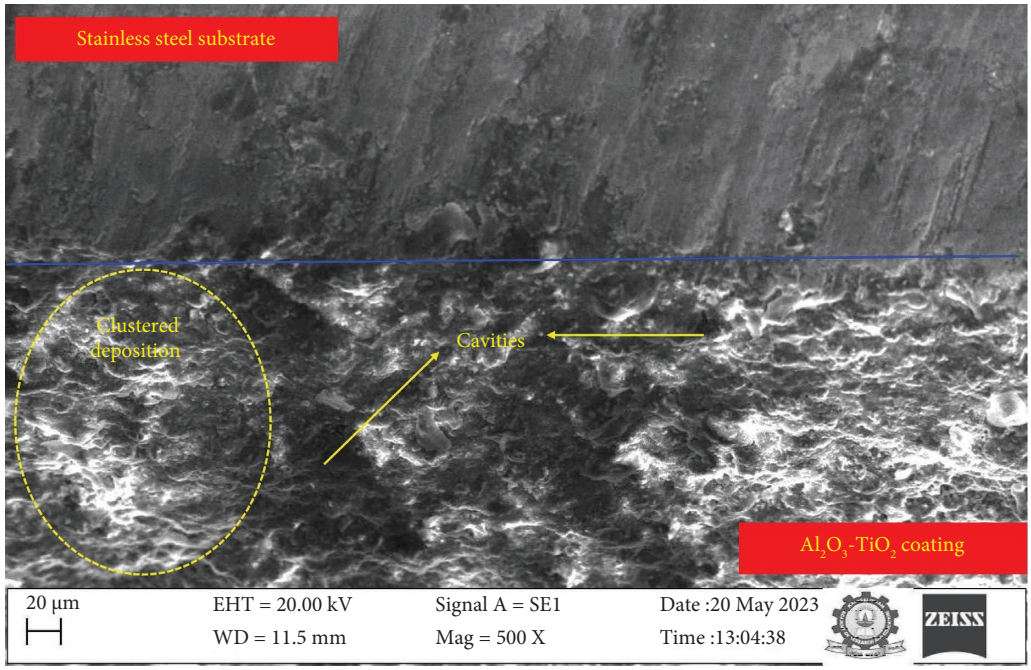

Figure 5: Cross-sectional SEM image of coated stainless steel.

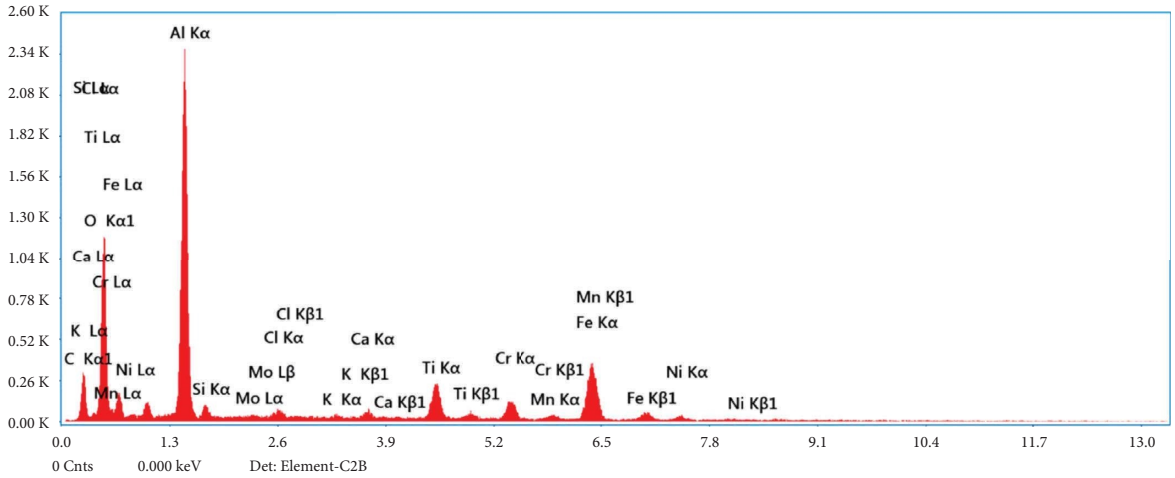

Figure 6: EDX spectra of coated stainless steel cross-sectional view.

Table 5: Elemental values obtained from EDX spectra.

Elements	Weight (%)
Carbon (C)	14.8
Oxygen (O)	26.8
Aluminum (Al)	25.7
Silicon (Si)	0.9
Molybdenum (Mo)	0.5
Chloride (Cl)	0.8
Potassium (K)	0.4
Calcium (Ca)	1.0
Titanium (Ti)	5.6
Chromium (Cr)	4.1
Manganese (Mn)	0.8
Iron (Fe)	16.6
Nickel (Ni)	2.1

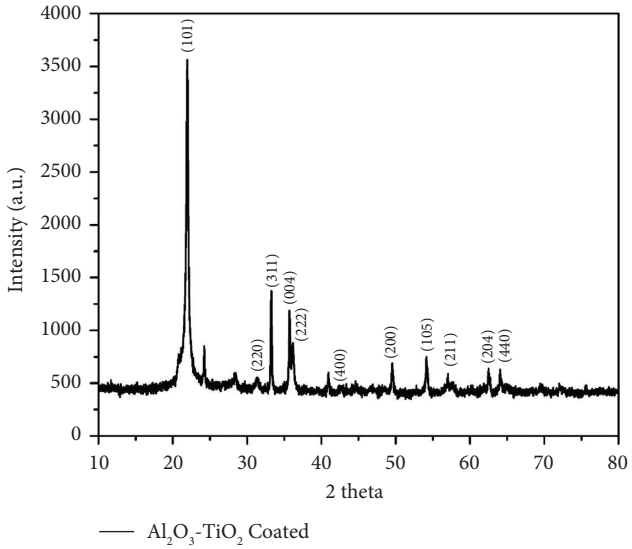

Figure 7: X-ray diffraction pattern of coated stainless steel.

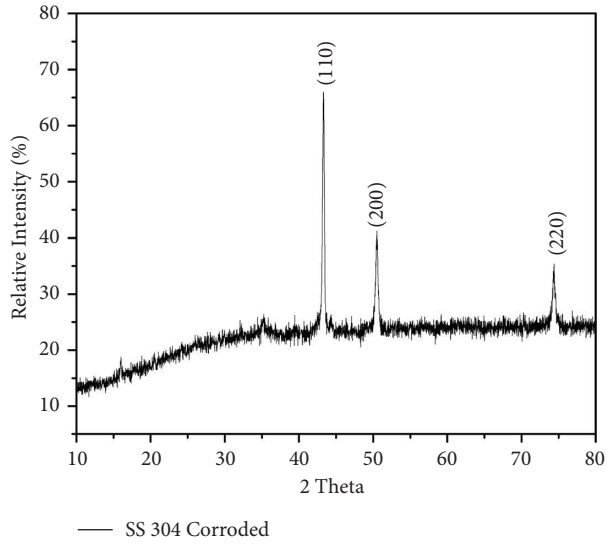

Figure 8: X-ray diffraction pattern of corroded stainless steel.

immersions, some corrosion was observed on the surface; however, the surface of coated SS looked better than that of uncoated SS. Thus, it was predicted based on immersion test that the alumina-titania coating enhanced corrosion resistance of SS [39, 40].

The corrosion rate is calculated using equation (1). The corrosion rate with respect to the exposure time is represented in Figure 11:

$$\text{corrosion rate (mm/year)} = 87.6 \times \frac{W}{\text{DAT}}, \quad (1)$$

where W is weight loss in milligrams, D is stainless steel density (8 g/cm^3), A is the area of the sample (48 cm^2), and T is the exposure time in hours.

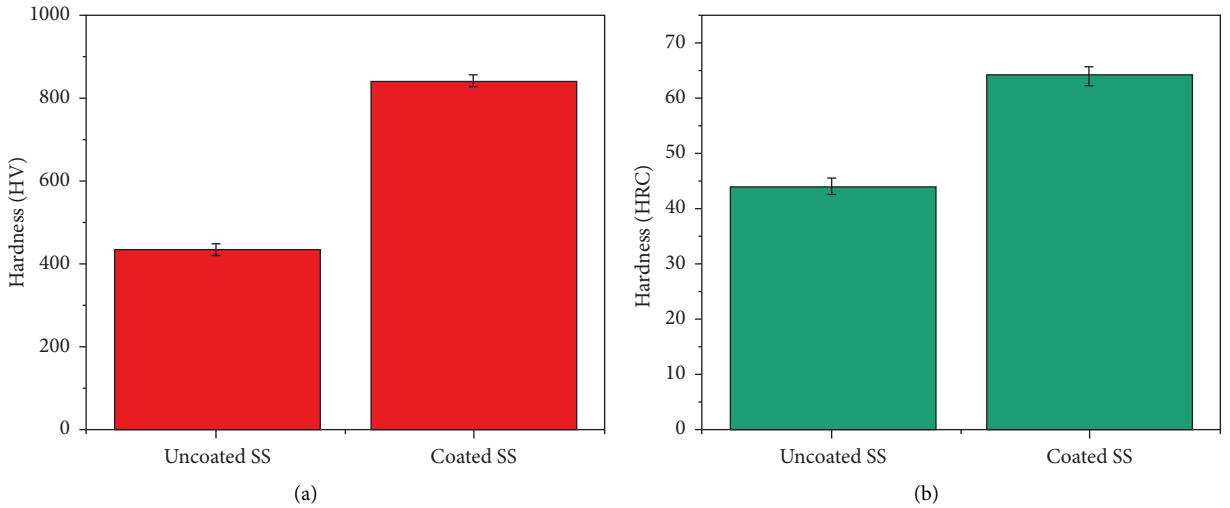

Figure 9: The hardness of the surface on (a) the HV scale and (b) the HRC scale.

Table 6: Test observation of the salt spray method.

Materials	Time interval	Observation
Uncoated stainless steel	At 12 hours	Negligible corrosion
Uncoated stainless steel	At 24 hours	Corrosion occurred
Coated stainless steel	At 12 hours	No corrosion
Coated stainless steel	At 24 hours	No corrosion

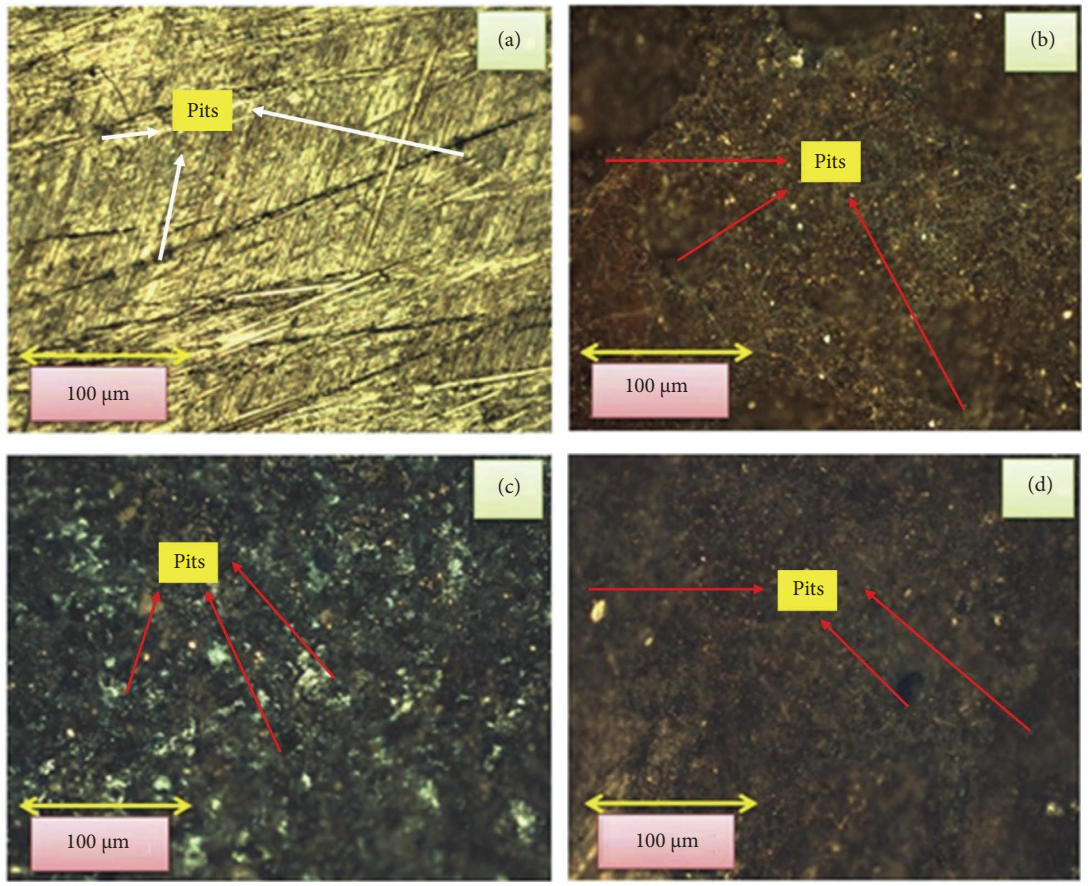

Figure 10: Microscopic images of (a) SS, (b) corroded SS, (c) coated SS, and (d) coated SS after corrosion.

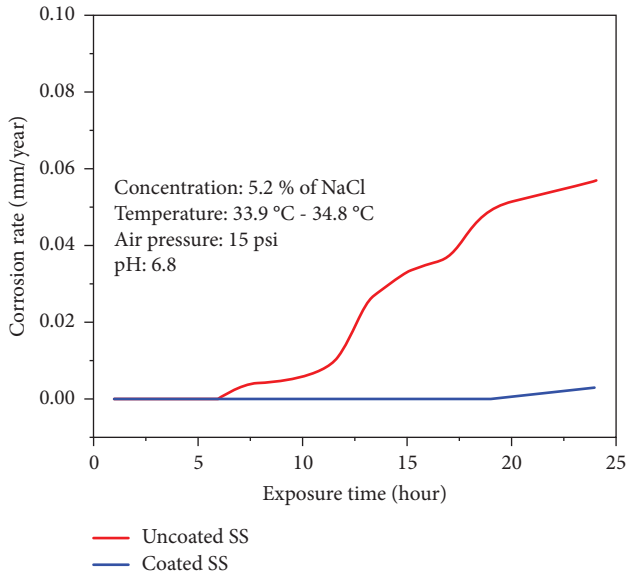

Figure 11: Rate of corrosion with the exposure time.

4. Conclusion

Alumina-titania was deposited on the stainless steel by the detonation spray method. This study provides the following conclusions:

(i) The SEM images also confirmed this fact and suggested that a rough coating of alumina-titania was deposited on stainless steel.

(ii) The X-ray diffraction peaks suggested that alumina-titania, alumina, and titania were detected on the coated stainless steel surface.

(iii) Micro Vickers hardness test results showed that the coated stainless steel has a higher hardness than the uncoated stainless steel. From these results, it is observed that the hardness of coated stainless steel is increased by 43.51% than uncoated stainless steel.

(iv) From the salt spray corrosion test, it could be concluded that the uncoated stainless steel had less corrosion resistance than the coated stainless steel. In other words, it could be said that the applied coating was highly resistant to oxide formation caused by salt spraying.

(v) The immersion test also confirmed this fact. As an overall conclusion, it could be stated that the alumina-titania coating increased the corrosion resistance of stainless steel against chloride ions.

Nomenclature

Al_2O_3: Alumina
TiO_2: Titania
mm: Millimeter
ml: Milliliter
kV: Kilovolts
°C: Degree Celsius
NaCl: Sodium chloride
psi: Pounds per square inch
μm: Micrometer
a.u: Atomic unit

Abbreviations

SEM: Scanning electron microscope
D-gun: Detonation gun
XRD: X-ray diffraction
SS: Stainless steel
MMC: Metal matrix composite
ASTM: American Society for Testing Materials
HV: Vickers hardness
HRC: Rockwell hardness C
VHN: Vickers hardness number
IS: International standard
HVOF: High-velocity oxy-fuel.

Data Availability

The data used to support the findings of this study are available on request.

Conflicts of Interest

The authors declare that they have no conflicts of interest.

Authors' Contributions

All the authors significantly contributed in this manuscript. A. Surya was involved in investigation, conceptualization, methodology, and writing the original draft. R. Prakash and P. Senthil Kumar were involved in conceptualization, methodology, funding acquisition, validation, and supervision. G. Bharath Balji was involved in funding acquisition, formal analysis, validation, and data curation.

References

[1] S. Zhang, S. Wang, C. L. Wu, C. H. Zhang, M. Guan, and J. Z. Tan, "Cavitation erosion and erosion-corrosion resistance of austenitic stainless steel by plasma transferred arc welding," *Engineering Failure Analysis*, vol. 76, pp. 115–124, 2017.

[2] W. Wan, J. Xiong, Y. Li, Q. Tang, and M. Liang, "Erosion-corrosion behavior of Ti (C, N)-based cermets containing different secondary carbides," *International Journal of Refractory Metals and Hard Materials*, vol. 66, pp. 180–187, 2017.

[3] J. Aguirre and M. Walczak, "Effect of dissolved copper ions on erosion–corrosion synergy of X65 steel in simulated copper tailing slurry," *Tribology International*, vol. 114, pp. 329–336, 2017.

[4] K. Selvam, A. Ayyagari, H. S. Grewal, S. Mukherjee, and H. S. Arora, "Enhancing the erosion-corrosion resistance of steel through friction stir processing," *Wear*, vol. 386-387, pp. 129–138, 2017.

[5] U. Ahmed, L. Yi, L. F. Fei, M. Yasir, C. J. Li, and C. X. Li, "Enhancement of corrosion resistance and tribological properties of LA43M Mg alloy by cold-sprayed aluminum coatings reinforced with alumina and carbon nanotubes," *Journal of Thermal Spray Technology*, vol. 30, no. 3, pp. 668–679, 2021.

[6] F. G. Ferré, A. Mairov, D. Iadicicco et al., "Corrosion and radiation resistant nanoceramic coatings for lead fast reactors," *Corrosion Science*, vol. 124, pp. 80–92, 2017.

[7] A. Goyal, R. Singh, and G. Singh, "Study of high-temperature corrosion behavior of D-gun spray coatings on ASTM-SA213, T-11 steel in molten salt environment," *Materials Today: Proceedings*, vol. 4, no. 2, pp. 142–151, 2017.

[8] S. Singh, K. Goyal, and R. Goyal, "Performance of Cr₃C₂-25(Ni-20Cr) and Ni-20Cr Coatings on T91 Boiler Tube Steel in Simulated Boiler Environment at 900&#8451," *Chemical and Materials Engineering*, vol. 4, no. 4, pp. 57–64, 2016.

[9] C. L. Wu, S. Zhang, C. H. Zhang, H. Zhang, and S. Y. Dong, "Phase evolution and cavitation erosion-corrosion behavior of FeCoCrAlNiTix high entropy alloy coatings on 304 stainless steel by laser surface alloying," *Journal of Alloys and Compounds*, vol. 698, pp. 761–770, 2017.

[10] Y. Huang, X. Ding, C. Q. Yuan, Z. K. Yu, and Z. X. Ding, "Slurry erosion behaviour and mechanism of HVOF sprayed micro-nano structured WC-CoCr coatings in NaCl medium," *Tribology International*, vol. 148, Article ID 106315, 2020.

[11] N. V. Abhijith, D. Kumar, and D. Kalyansundaram, "Development of single-stage TiNbMoMnFe high-entropy alloy coating on 304L stainless steel using HVOF thermal spray," *Journal of Thermal Spray Technology*, vol. 31, no. 4, pp. 1032–1044, 2022.

[12] M. Dawood and P. K. Sinha, "Experimental investigation and analysis of stainless steel 316L by salt spray test method for corrosion behavior," in *Recent Advances in Mechanical Engineering: Select Proceedings of ITME 2019*, pp. 385–393, Springer Singapore, Singapore, 2021.

[13] Y. Lu, Z. Chen, C. Wang et al., "Protection of 304 stainless steel by nano-modified silicone coating in cyclically alternate corrosion environment," *Corrosion Science*, vol. 190, Article ID 109712, 2021.

[14] Z. Ren and F. Ernst, "Stress–corrosion cracking of AISI 316L stainless steel in seawater environments: effect of surface machining," *Metals*, vol. 10, no. 10, p. 1324, 2020.

[15] F. Cao, Z. Shi, G. L. Song, M. Liu, and A. Atrens, "Corrosion behaviour in salt spray and in 3.5% NaCl solution saturated with $Mg(OH)_2$ of as-cast and solution heat-treated binary Mg–X alloys: X= Mn, Sn, Ca, Zn, Al, Zr, Si, Sr," *Corrosion Science*, vol. 76, pp. 60–97, 2013.

[16] R. Li, S. Wang, D. Zhou, J. Pu, M. Yu, and W. Guo, "A new insight into the NaCl-induced hot corrosion mechanism of TiN coatings at 500 °C," *Corrosion Science*, vol. 174, Article ID 108794, 2020.

[17] Y. Baoxu, C. Haixiang, and K. Dejun, "Effects of laser remelting on salt spray corrosion behaviors of arc-sprayed Al coatings in 3.5% NaCl sea environment," *Transactions of the Indian Institute of Metals*, vol. 71, no. 3, pp. 617–625, 2018.

[18] I. D. Kuchumova, M. A. Eryomina, N. V. Lyalina et al., "Structural features and corrosion resistance of Fe66Cr10Nb5B19 metallic glass coatings obtained by detonation spraying," *Journal of Materials Engineering and Performance*, vol. 31, no. 1, pp. 622–630, 2022.

[19] G. Kaya, B. Gunhan, I. O. Ozer, and H. B. Poyraz, "Production of TiO_2 coated α-Al_2O_3 platelets by flame spray pyrolysis and their characterization," *Ceramics International*, vol. 46, no. 16, pp. 25512–25519, 2020.

[20] P. U. C. Rao, P. S. Babu, D. S. Rao, S. G. Krishna, and K. V. Rao, "Effect of tribo-layer on the sliding wear behavior of detonation sprayed alumina-titania coatings," in *Intelligent Manufacturing and Energy Sustainability: Proceedings of ICIMES 2019*, p. 289, Springer, Singapore, 2020.

[21] M. Djendel, O. Allaoui, and R. Boubaaya, "Characterization of alumina-titania coatings produced by atmospheric plasma spraying on 304 SS steel," *Acta Physica Polonica A*, vol. 132, no. 3, pp. 538–540, 2017.

[22] T. Peat, A. M. Galloway, A. I. Toumpis, and D. Harvey, "Evaluation of the synergistic erosion-corrosion behaviour of HVOF thermal spray coatings," *Surface and Coatings Technology*, vol. 299, pp. 37–48, 2016.

[23] V. Sharma, M. Kaur, and S. Bhandari, "Development and characterization of high-velocity flame sprayed Ni/TiO_2/Al_2O_3 coatings on hydro turbine steel," *Journal of Thermal Spray Technology*, vol. 28, no. 7, pp. 1379–1401, 2019.

[24] H. S. Grewal, A. Agrawal, H. Singh, and B. A. Shollock, "Slurry erosion performance of Ni-Al_2O_3 based thermal-sprayed coatings: effect of angle of impingement," *Journal of Thermal Spray Technology*, vol. 23, no. 3, pp. 389–401, 2014.

[25] M. Amiriafshar, M. Rafieazad, X. Duan, and A. Nasiri, "Fabrication and coating adhesion study of superhydrophobic stainless steel surfaces: the effect of substrate surface roughness," *Surfaces and Interfaces*, vol. 20, Article ID 100526, 2020.

[26] W. B. Liao, Z. X. Wu, W. Lu et al., "Microstructures and mechanical properties of CoCrFeNiMn high-entropy alloy coatings by detonation spraying," *Intermetallics*, vol. 132, Article ID 107138, 2021.

[27] J. Jhansi, S. Santhi, P. V. S. Lakshmi Narayana, and B. K. Deogade, "Detonation gun spray coatings on martensitic stainless Steels," in *Recent Advances in Manufacturing, Automation, Design and Energy Technologies: Proceedings from ICoFT 2020*, pp. 85–93, Springer, Singapore, 2022.

[28] A. Singh, K. Goyal, R. Goyal, and B. Krishan, "Hot corrosion behaviour of different ceramics coatings on boiler tube steel at 800 °C temperature," *Journal of Bio-and Tribo-Corrosion*, vol. 7, pp. 21–29, 2021.

[29] I. D. Kuchumova, I. S. Batraev, A. V. Ukhina et al., "Processing of Fe-based alloys by detonation spraying and spark plasma sintering," *Journal of Thermal Spray Technology*, vol. 30, no. 6, pp. 1692–1702, 2021.

[30] S. M. Gateman, I. Halimi, A. R. Costa Nascimento et al., "Using macro and micro electrochemical methods to understand the corrosion behavior of stainless steel thermal spray coatings," *Npj Materials Degradation*, vol. 3, no. 1, p. 25, 2019.

[31] N. Kantay, B. Rakhadilov, S. Kurbanbekov, D. Yeskermessov, G. Yerbolatova, and A. Apsezhanova, "Influence of detonation-spraying parameters on the phase composition and tribological properties of Al_2O_3 coatings," *Coatings*, vol. 11, no. 7, p. 793, 2021.

[32] J. Cheng, Y. Ge, B. Wang et al., "Microstructure and Tribocorrosion behavior of Al_2O_3/Al composite coatings: role of Al_2O_3 addition," *Journal of Thermal Spray Technology*, vol. 29, no. 7, pp. 1741–1751, 2020.

[33] K. A. Habib, J. J. Saura, C. Ferrer, M. S. Damra, and I. Cervera, "Oxidation behaviour at 1123 K of AISI 304-Ni/Al-Al_2O_3/TiO_2 multilayer system deposited by flame spray," *Revista de Metalurgia*, vol. 47, no. 2, pp. 126–137, 2011.

[34] J. Zhou, K. Sun, S. Huang et al., "Fabrication and property evaluation of the Al_2O_3-TiO_2 composite coatings prepared by plasma spray," *Coatings*, vol. 10, no. 11, p. 1122, 2020.

[35] T. Sathish, V. Mohanavel, T. Arunkumar et al., "Investigation of mechanical properties and salt spray corrosion test

parameters optimization for Aa8079 with reinforcement of Tin+ Zro2," *Materials*, vol. 14, no. 18, p. 5260, 2021.

[36] R. Krishnan, S. Manivannan, P. B. Patel et al., "Studies on corrosion behavior of Mg-Al-Zn-RE cast alloy with powder-coated Al and CED Mg by salt spray test, immersion test, and electrochemical test," *International Journal of Chemical Engineering*, vol. 2022, Article ID 1891419, 11 pages, 2022.

[37] Z. Wen and K. Dejun, "Salt spray corrosion and electrochemical corrosion characteristics of CAIP and LTPN fabricated AlCrN/NL composite coating," *Materials Research Express*, vol. 6, no. 4, Article ID 046413, 2019.

[38] H. Chen, W. Gao, T. Liu, W. Lin, and M. Li, "An experimental study on the effect of salt spray testing on the optical properties of solar selective absorber coatings produced with different manufacturing technologies," *International Journal of Energy and Environmental Engineering*, vol. 10, no. 2, pp. 231–242, 2019.

[39] R. K. Pandey, R. Mishra, G. Ji, and R. Prakash, "Corrosion prevention of commercial alloys by air-water interface grown, edge on oriented, ultrathin squaraine film," *Scientific Reports*, vol. 9, Article ID 13488, 2019.

[40] G. Ji, G. Ji, and R. Prakash, "Composites of Donor-π-Acceptor type configured organic compound and porous ZnO nano sheets as corrosion inhibitors of copper in chloride environment," *Journal of Molecular Liquids*, vol. 280, pp. 160–172, 2019.